

## NOTE

## Direct aperture optimization of breast IMRT and the dosimetric impact of respiration motion

Guowei Zhang, Ziping Jiang, David Shepard, Bin Zhang and Cedric Yu

Department of Radiation Oncology, University of Maryland School of Medicine, Baltimore, MD 21201, USA

E-mail: [gzhan002@umaryland.edu](mailto:gzhan002@umaryland.edu)

Received 9 June 2006, in final form 21 August 2006

Published 3 October 2006

Online at [stacks.iop.org/PMB/51/N357](http://stacks.iop.org/PMB/51/N357)

### Abstract

We have studied the application of direct aperture optimization (DAO) as an inverse planning tool for breast IMRT. Additionally, we have analysed the impact of respiratory motion on the quality of the delivered dose distribution. From this analysis, we have developed guidelines for balancing the desire for a high-quality optimized plan with the need to create a plan that will not degrade significantly in the presence of respiratory motion. For a DAO optimized breast IMRT plan, the tangential fields incorporate a flash field to cover the range of respiratory motion. The inverse planning algorithm then optimizes the shapes and weights of additional segments that are delivered in combination with the open fields. IMRT plans were generated using DAO with the relative weights of the open segments varied from 0% to 95%. To assess the impact of breathing motion, the dose distribution for the optimized IMRT plan was recalculated with the isocentre sampled from a predefined distribution in a Monte Carlo convolution/superposition dose engine with the breast simulated as a rigid object. The motion amplitudes applied in this study ranged from 0.5 to 2.0 cm. For a range of weighting levels assigned to the open field, comparisons were made between the static plans and the plans recalculated with motion. For the static plans, we found that uniform dose distributions could be generated with relative weights for the open segments equal to and below 80% and unacceptable levels of underdosage were observed with the weights larger than 80%. When simulated breathing motion was incorporated into the dose calculation, we observed a loss in dose uniformity as the weight of the open field was decreased to below 65%. More quantitatively, for each 1% decrease in the weight, the per cent volume of the target covered by at least 95% of the prescribed dose decreased by approximately 0.10% and 0.16% for motion amplitudes equal to 1.5 cm and 2.0 cm, respectively. When taking into account the motion effects, the most uniform and conformal dose distributions were achieved when the open segment weights were in the range of 65–80%. Within this range, high-quality IMRT plans were produced for

each case. The study demonstrates that DAO with tangential fields provides a robust and efficient technique for breast IMRT planning and delivery when the open segment weight is selected between 65% and 80%.

(Some figures in this article are in colour only in the electronic version)

## 1. Introduction

In creating a treatment plan for breast IMRT, the goal is to achieve a uniform dose distribution throughout the breast while minimizing the dose to the underlying lung, heart and surrounding normal tissues. Inverse planning for breast irradiation is challenging because the breast moves with the patient's breathing. In a traditional tangential breast irradiation, a flash field, defined as an open field that covers the whole breast plus certain margins, is added to each beam to ensure that the breast will not move out of the beam during delivery. Inverse planning is complicated by the fact that in the anterior direction the breast is surrounded not by normal tissue but rather by air.

Various approaches have been introduced for breast irradiation. The conventional three-dimensional planning approach using two parallel-opposed wedged tangential fields can result in significant dose heterogeneity, as large as 15% to 20% (Buchholz *et al* 1997, Cheng *et al* 1994, Kestin *et al* 2000). The forward planning technique (Kestin *et al* 2000) can improve dose uniformity but it requires more steps to generate a plan and the planning system has only the function to change the segment weights and this limited freedom could lead to sub-optimal plans. Due to planning complications, the use of other approaches as proposed by Li *et al* (2004) and by Mayo *et al* (2005) to meet clinical needs is challenging.

Due to patient movement, inaccurate patient positioning and organ motion, the patient's anatomy and position during the course of radiation therapy usually varies from simulation CT images. These variations may result in the actual received absorbed dose distribution differing from the planned absorbed dose distribution (Langen and Jones 2001). During normal breathing in breast irradiation, the posterior field border and the chest wall move, and thus, the relative position and even the shape of the breast change. Since the simulation CT images are snapshots of the anatomy during the breathing cycle, the dose distribution of a computer-generated treatment plan can never be faithfully delivered to the patient. For conventional treatment with wedged tangential fields, the breathing motion degrades the dose distribution by broadening the beam penumbra at the edge of the fields, which lowers the dose to the breast near the posterior field border and increases dose to the underlying lung and heart.

With intensity modulation, the dosimetric impact of respiratory motion is more complicated due to the aliasing effect of patient motion and the motion of the radiation fields. Unlike treatments with wedges, the interplay of patient motion and moving segments in IMRT can also lead to hot and cold spots inside the breast. When patient motion is ignored in the planning, the magnitude of the intensity variations in a target could be greater than 100% of the desired beam intensity (Yu *et al* 1998). The difference between the planned and expected dose distributions is found to increase with the amplitude of respiratory motion and the degradation is severe for heavy breathing, but is not statistically significant for shallow breathing or normal breathing (George *et al* 2003).

To reduce the effects of breathing motion, several strategies including gating and tracking have been proposed. Using the active breathing control (ABC) device, IMRT plans can be

delivered to breast patients (Frazier *et al* 2004, Remouchamps *et al* 2003a, 2003b, 2003c, Vicini *et al* 2004, Wilson *et al* 2003, Wong *et al* 1999) with the beam on only at the specific breathing phase used for planning. In motion adaptive radiotherapy as proposed by Keall *et al* (2001), the target motion due to respiration was superimposed onto the beam originally planned for delivery, and the MLC leaf positions were changed in a dynamic fashion with respect to the isocentre. When the target motion was ignored, the dose was smeared out and the studied case showed that a major dose peak was underestimated by 20%.

The DAO planning technique uses a simulated annealing algorithm that directly optimizes the shapes and relative weights of the apertures (Shepard *et al* 2002). The key feature of DAO is that all of the machine delivery constraints are included in the optimization, eliminating the need for leaf sequencing. Consequently, the planner can pre-specify the number of allowable apertures per beam. At the start of the optimization, all segments in a given beam are initialized to have the same weight and same shape, which encompasses the beam's-eye-view of the PTV. The initial shape, which also serves as the outer boundary of all segments, can also be manually defined. In addition to the definition of dosimetric constraints, the user is also given the option to keep the initial segment shape as the first segment in the beam, while the shapes of all other segments and the weights of all the segments are optimized. The relative weight, which is defined as the percentage of the monitor units to be delivered from that beam direction, of the first segment to the total weight of all segments of the same beam is held at a fixed value. All the segments of each beam, including the first open segment, use the same set of pencil beams. The user specifies the maximum number of apertures to be optimized and delivered for each beam, and also defines the relative weight of the open segment.

From clinical experience, we realized that DAO should be well suited for planning breast IMRT. Although the DAO technique cannot eliminate the impact of breathing motion, we can maximize the weight of the open segment to reduce these effects. This is because each open flash segment covers the entire breast for the whole breathing cycle. If, however, the weight assigned to the open segment is too large, it limits the ability to modulate the intensity of the beam and therefore sacrifices the plan quality. One task of this study was to find the optimal range of weightings for this open segment so that we can provide guidelines for balancing the need for dose uniformity with the desire to reduce the impact of respiratory motion.

In this paper, we introduce a new, robust and DAO based inverse planning technique for breast IMRT. The purpose of this study is two-fold: (1) to evaluate the clinical merit of the DAO strategy and (2) to study the relationship between the effects of motion and the relative weightings of the open flash field and develop guidelines for minimizing plan degradation due to breathing motion.

## 2. Methods and materials

### 2.1. Beam definition and volume delineation

The tangential fields were set up using CT-simulation as in conventional treatment planning. The beam arrangement, including the isocentre, gantry and collimator angles, and the field borders were designed to (1) cover the whole breast tissue with a 2 cm margin in both superior and inferior directions, (2) provide a 2 cm flash beyond the skin surface anteriorly in the beam's-eye-view and (3) perfectly align the posterior boundaries of the two tangential fields with the collimator angle set to minimize the volume of lung in the fields. Unlike conventional treatment planning for breast, the PTV must be delineated on the CT data set for inverse planning to proceed. The PTV was contoured to cover the clinically determined breast tissue and superficially it was defined 5 mm inside of the skin surface so that the lower doses in

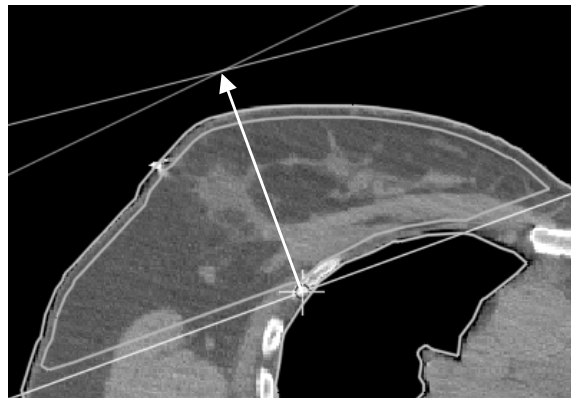


**Figure 1.** Tangential beam set-up. The arrow represents that patient moving direction.

the build-up region are not considered in the optimization process. Figure 1 shows the beam set-up.

### 2.2. DAO based planning systems

Using the DAO planning technique, we have developed a strategy that enforces an open flash segment covering the entire breast and a portion of air beyond the anterior contour of breast in the beam's-eye-view while optimizing the shapes and weights of the IMRT segments. A commercial inverse planning system, Prowess Panther<sup>TM</sup> (Prowess, Inc., Chico, CA), was used for this study. The system employs the DAO algorithm for dose optimization that was developed at our institution (Earl *et al* 2003, Shepard *et al* 2002). Because the planning system operates on a single static CT image set, the optimized weight for the open segment without considering motion may not be optimal when breast motion is considered. In this study, DAO optimizations for a typical cancer patient were conducted with varying open segment ratios using identical objectives and constraints. The planning parameters were selected such that all plans provided a fixed level of overdose. Therefore, in comparing plans, the focus was primarily on the dose coverage and the degree of underdosage.

### 2.3. Patient motion modelling

An important consideration for IMRT is the relationship between MLC motion and CTV motion (Keall *et al* 2001, Ozhasoglu and Murphy 2002) and the impact of this interplay on unplanned over- or underdosage of PTV (George *et al* 2003). A breast IMRT plan should be evaluated in terms of the moving patient, or at least the moving breast. In this study, the plan quality has been investigated by comparing the dose distributions of the plan for the static breast with plans that account for the breast motion. All plans were optimized using Prowess TPS, and the final dose was calculated using an external Monte Carlo based dose engine developed at our institution (Naqvi *et al* 2003). The dose engine superimposes energy deposition kernels using the Monte Carlo superposition technique, and the histories are tracked on a photon-by-photon basis. For each history, the isocentre position is sampled randomly from the predefined motion trajectory (Naqvi and D'Souza 2005).

Note that the Monte Carlo dose calculation ignored the timing of the delivery of individual segments, and therefore the resultant dose distribution theoretically represented the average

effects of breast motion over an infinite number of fractions and the interplay between MLC motion and the target movement appears not to be reflected in the dose distribution. However Naqvi and D'Souza (2005) demonstrated that a ten-fraction average is close to the calculated infinite fraction average. In the test, they obtained ten separate film measurements of an IMRT plan delivered on a phantom moving sinusoidally, with each fraction starting with a random phase. For 2 cm motion amplitude, they found that the average of the ten film measurements gave an agreement with the calculated infinite fraction average to within 2 mm in the isodose lines. A typical treatment course is designed to deliver 45 to 50 Gy to the whole breast with 25 fractions. Within a less than 2 mm statistical error, the calculated infinite fraction average well represents the dose distribution that the patient actually will receive from the 25 fractions provided that the condition which the calculation is based on adequately and sufficiently reflects the actual clinical circumstances.

Incorporating organ motion into dose calculation in general can also be accomplished by applying a convolution procedure with the motion pattern onto fluence (Naqvi and D'Souza 2005) or onto the dose that has been calculated without patient motion as described by Lujan *et al* (1999). The reason we take the former approach, i.e., incorporating patient motion with the fluence into the dose calculation, is that Monte Carlo by its nature provides this convenience given the fact that we have the source code and an interface to do this. Thus in this study the inclusion of the patient motion in the dose calculation does not need any special module, algorithm and program except for the motion pattern itself. The extra calculation power for calculating the isocentre shift in each history is negligible when comparing it with the complexity of the dose calculation.

As for the motion pattern, Kubo and Hill (1996) and George *et al* (2003) observed that the chest walls of breast patients move outward from the original position, but the motion is almost constant along the superior–inferior edge of the radiation field, and the movement pattern is a sine-like curve with a larger displacement for inhalation and a smaller displacement for exhalation. Throughout this study, we assume that the motion occurs only in the anterior–posterior and the medial–lateral directions, i.e., there is no superior–inferior motion and no rotation. As a result, the movement of the breast is in a single direction, which is further assumed to be perpendicular to the posterior boundary of the beams, as indicated by the arrow in figure 1. Another assumption is that the PTV is a moving rigid object, i.e., the intrafraction motion does not deform the patient geometry.

With these assumptions in mind, the isocentre displacement in the dose calculation was defined as follows:

$$X = A * d_x * p$$

and

$$Y = A * d_y * p$$

where

- $X$  and  $Y$  are the displacements in the lateral and AP directions, respectively;
- $A$  is the amplitude of motion along the direction of motion. The maximum displacement in one component direction (either AP or lateral) observed by other researchers ranges from 1.5 to 2.0 cm (George *et al* 2003, Kubo and Hill 1996). In this study, the maximum motion amplitude along the moving direction, i.e.,  $A$  is up to 2.0 cm;
- $d_x$  and  $d_y$  are the directional components of the unit motion in the lateral and AP directions so that  $\sqrt{d_x^2 + d_y^2} = 1$  holds, and the direction of motion is perpendicular to the posterior border of the beams, as described previously; and

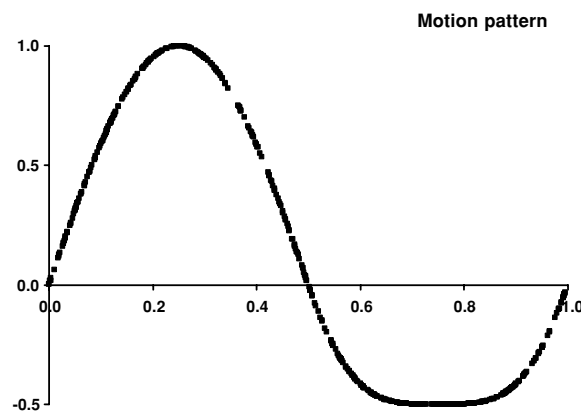


Figure 2. Motion pattern.

- $p$  is the moving pattern that is a temporal function of displacement and is represented by a random number. It is defined as

$$\begin{aligned} & \sin(2\pi * r), \quad \text{when } r < 0.5 \text{ (inhalation), and} \\ & 0.5 * (2.0 - |\sin(2\pi * r)|) * \sin(2\pi * r), \quad \text{when } r \geq 0.5 \text{ (exhalation),} \end{aligned}$$

where  $r$  is a random number and it is uniformly distributed in the range from 0 to 1. The displacement is 0.5 and 1.0 at the end of the inhalation and exhalation, respectively. The ratio of the maximum displacements at the two ends was designed so as to match the clinical data, as reported in the literature (Frazier *et al* 2004).

The motion pattern is designed so that it is in line with the observations of other researchers (Frazier *et al* 2004, George *et al* 2003, Lujan *et al* 1999, Kubo and Hill 1996). Figure 2 shows the pattern of movement with the motion amplitude normalized to 1. The patient moves with the same displacement but in the opposite direction when the isocentre is taken as reference. To demonstrate how this model works, a simple  $1 \times 2 \text{ cm}^2$  rectangular beam was calculated on a flat-water phantom with 95 cm SSD and 100 MU irradiation. A motion amplitude of 1.5 cm was applied in the Monte Carlo superposition dose calculation. Figures 3(a) and (b) show the isodose lines of 2%, 5%, 20% and 60% at depth of 5 cm for the dose calculation without motion and with a motion amplitude of 1.5 cm, respectively. Since a scale of 100% equal to 100 cGy is used in the diagram, these numbers also represent the dose in cGy. Figure 4 shows the corresponding dose profiles along the moving direction for the case without motion and the case with a motion amplitude of 1.5 cm. For a sine or sine-like motion pattern, the isocentre spends more time near the maximum displacement region than in the central region, and thus the dose near the edge of the motion is higher than that in the central area.

### 3. Results and discussion

A typical breast plan achieved with the DAO technique is presented. This right-breast case has a 25 cm distance of separation between the two cross points of the central axis of the beam and the skin and the volume of the whole breast PTV is  $2053 \text{ cm}^3$ . Figure 5 shows the segments and the intensity map of the IMRT plan for this case. The relative weight of

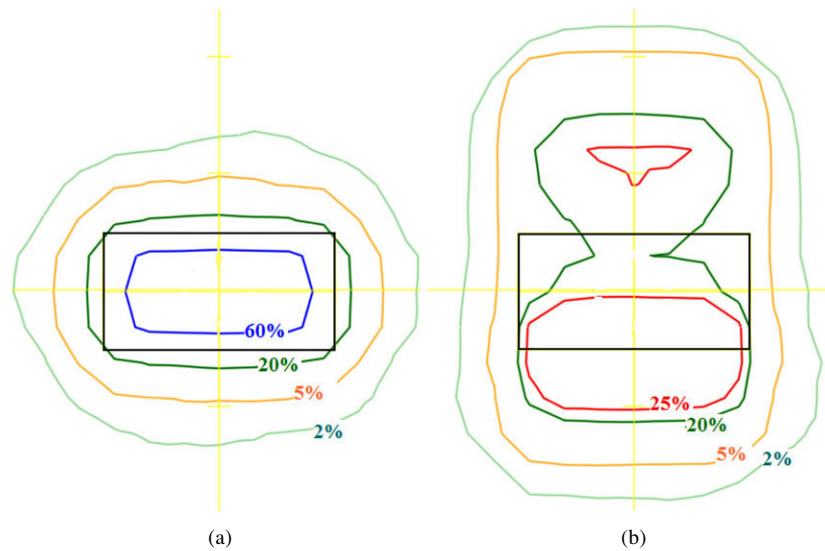


**Figure 3.** Isodose lines for a  $1 \times 2 \text{ cm}^2$  beam at a depth of 5 cm with motion amplitude equal to 0.0 cm (a) and 1.5 cm (b).

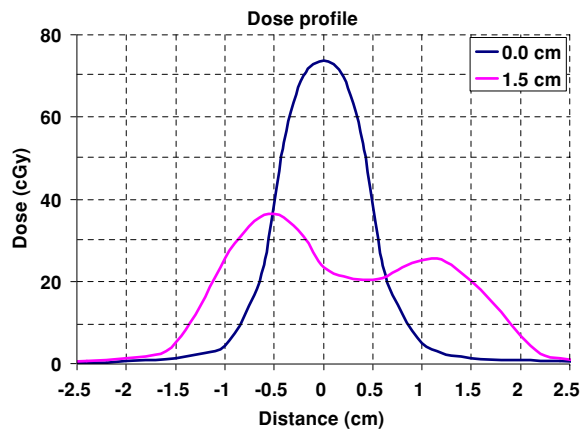


**Figure 4.** Dose profiles along the moving direction for a  $1 \times 2 \text{ cm}^2$  beam at a depth of 5 cm with motion amplitude equal to 0.0 cm and 1.5 cm.

the open segment was set to 80%. Additional plans were generated with more than seven segments per field, but those plans did not significantly improve dose coverage. We observed that when the number of segments exceeds a certain value, some of the segments are deleted at the end of the optimization because the MU assigned to these segments fell below the minimum threshold. Generally, plans created using the DAO approach require significantly fewer segments per beam, as compared with plans created through intensity map optimization followed by leaf-sequencing. This is because DAO incorporates all of the delivery constraints into the plan optimization. If too many segments are allowed in the DAO optimization, only a limited number of segments contribute to the optimized plan and all the extra segments are

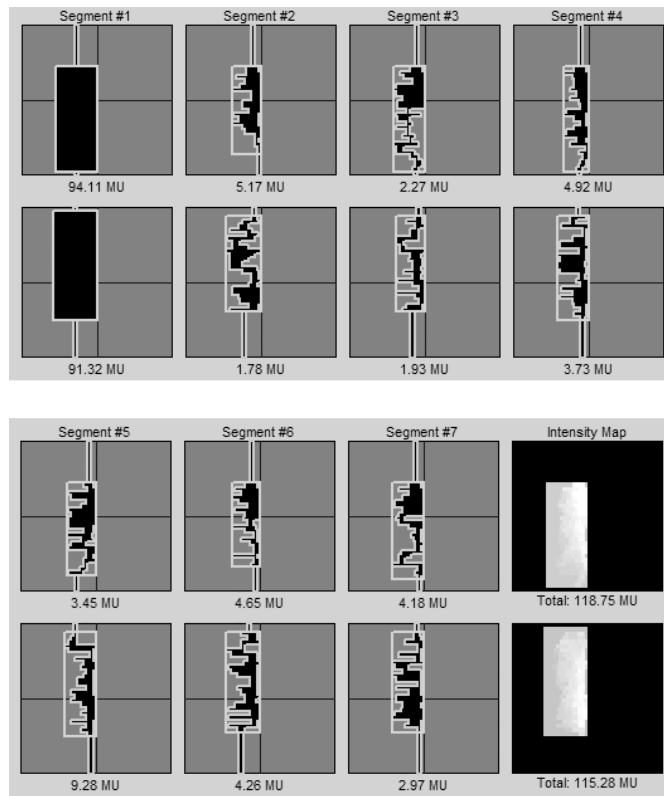


**Figure 5.** Segments and the intensity map and their MUs of an MLC based IMRT plan. The weight of the open field is 80%.

excluded from the plan. This exclusion of extra segments saves unnecessary delivery time, and also helps to reduce the final dose calculation errors that may result from ignoring collimator specific effects.

Figure 6 plots the DVHs for plans where the relative weights of the open segments are equal to 0%, 25%, 45%, 65%, 75%, 80%, 85%, 90% and 95% without considering patient motion. When the relative weight of the open field is larger than 80%, the dose distribution degrades significantly with each increase in the weight. The per cent volumes that are covered by at least 95% of the prescription dose are 93.8%, 90.1%, 88.8% and 82.5% for plans whose weight of the open field equal 80%, 85%, 90% and 95%, respectively. This demonstrates that when the weight is larger than 80%, the plans are not acceptable. The figure also shows that when the weight is below 85%, all plans provide acceptable coverage over the PTV and the differences in the degree of overdose are minor, and the dose distributions below 100% of the prescribed dose have no noticeable difference among the plans.

To evaluate the effects of breast motion on the quality of the dose distribution, plans with the open field assigned a weight ranging from 0 to 95% are recalculated using the patient motion simulation method as described previously. The motion amplitudes are 0.5, 1.0, 1.5 and 2.0 cm and the direction is perpendicular to the posterior border of the tangential beams, as shown in figure 1. Figure 7 shows the DVHs of the plans with 80% open field weighting and different motion amplitudes. When the motion amplitude is 0.5 cm, no noticeable degradation

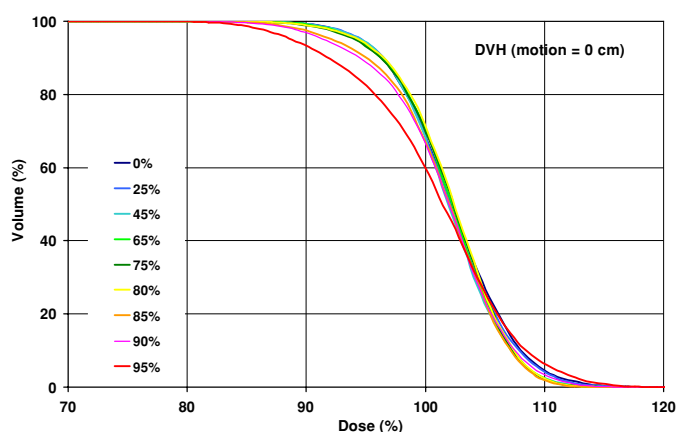


Figure 6. DVH diagrams of the plans without motion.

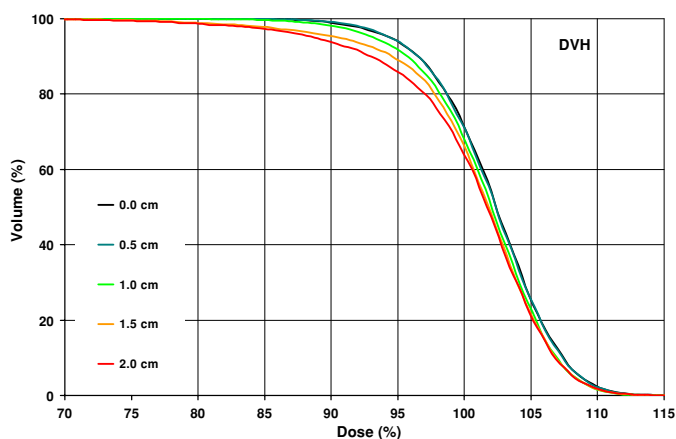


Figure 7. DVH diagrams of the plans with weight of the open field weight of 80% and motion amplitudes equal to 0.0 cm, 0.5 cm, 1.0 cm, 1.5 cm and 2.0 cm.

of dose distribution can be found. Dose coverage degradation increases with the increase in motion amplitude. All DVHs with patient motion included are under the DVH for the static patient throughout the entire dose range.

Figure 8 shows the DVHs of the plans with motion amplitudes of 0.5 cm but different open field weightings. As a benchmark, the DVH for the static plan with the open field weighting of 80% is also included in the comparison. Figures 9, 10 and 11 are the same as figure 9 except with motion amplitudes of 1.0, 1.5 and 2.0 cm, respectively. Comparing the difference between the static patient plan and the moving patient plan, it is not surprising that the plan degrades as the motion amplitude increases. Because our simulation sampled breast motion in a probabilistic manner, the effect of interplay between target motion and segment motion was averaged out. The overall effect of breast motion is the reduction of dose volume at all dose coverage levels. These observations are consistent with other researchers' results (George *et al* 2003, Xing *et al* 2000). For all motion amplitudes, the closest DVH to that of the static target is when the relative weighting of the open segment is at 80%,

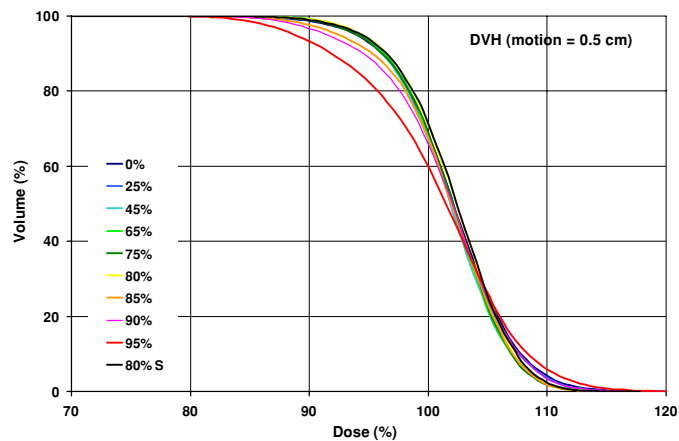


Figure 8. DVH diagrams of the plans with motion amplitude equal to 0.5 cm.

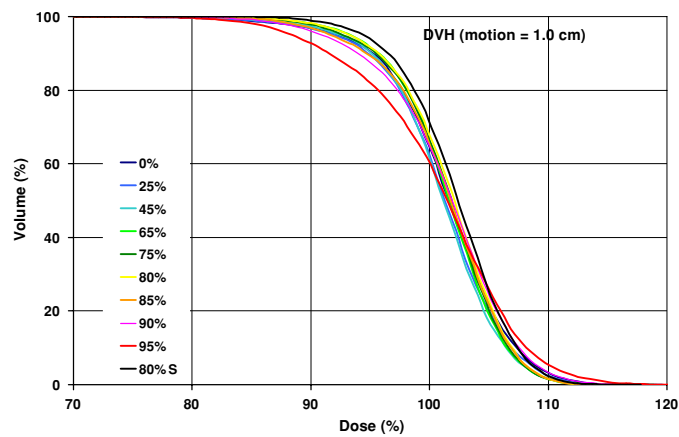


Figure 9. DVH diagrams of the plans with motion amplitude equal to 1.0 cm.

which is in line with or close to other researchers' observations (Frazier *et al* 2004, Mayo *et al* 2005). The dose distribution degrades when the weighting of the open segment deviates away from 80%. When the weight changes from 80% down to 0%, overdose has a slight but not significant difference, and the dose coverage in the range between 75% and 100% is degraded in varying degrees, depending on the motion amplitudes. For example, the per cent volumes of target covered at least by 95% of the prescribed dose in static plans for weight values from 0% to 80% are  $94.0 \pm 0.4\%$ . When considering patient motion, the corresponding per cent volumes with motion amplitude equal to 2.0 cm for the weight equal to 0%, 25%, 45%, 65%, 75% and 80% are 73.3%, 75.8%, 78.8%, 83.5%, 84.0% and 84.8%, respectively.

For better visualization, the percentages of the target volume covered by at least 95% of the prescribed dose for all weighting levels of the open field with all motion amplitudes are digitized from previous figures and are presented in figure 12. When there is no motion or the motion amplitude is less than or equal to 0.5 cm, all plans show similar coverage at 95% of

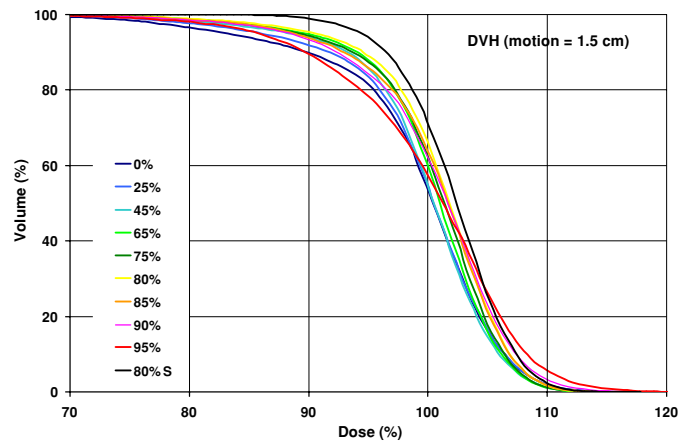


Figure 10. DVH diagrams of the plans with motion amplitude equal to 1.5 cm.

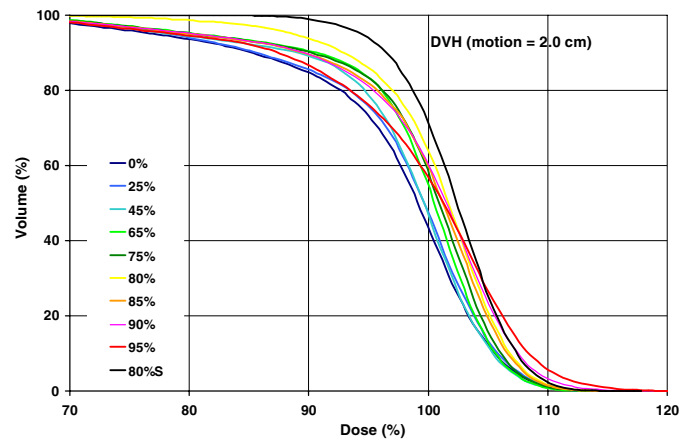
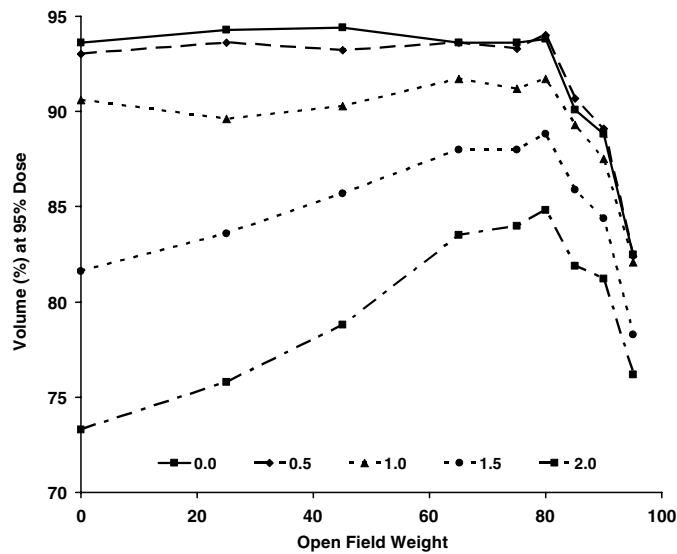


Figure 11. DVH diagrams of the plans with motion amplitude equal to 2.0 cm.

the prescribed dose for weights of the open segment up to 80%. The degradation of dose coverage with the open segment weighting greater than 80% simply reflects the fact that one cannot achieve uniform dose in the breast with open tangential fields. When the weight of the open field is below 65%, the dose coverage is decreased dramatically with the motion amplitude. For example, for a static patient having a weight of the open field equal to 0%, 25%, 45% and 65%, the dose coverage levels are 93.6%, 94.3%, 93.6% and 93.6%. For an amplitude of motion equal to 2.0 cm, the corresponding dose coverage degrades to 73.3%, 75.8%, 78.8% and 83.5%, respectively. As indicated in figure 12, a plateau is formed for the weight of the open field equal to 65%, 75% and 80% for plans with varying motion amplitudes. Within 1.3% error, the plans for these three weights give the highest dose coverage at 95% of the prescribed dose for all motion amplitudes. The results show that when considering the patient motion effects on dose distributions with motion amplitude up to 2.0 cm, the best plans are achieved by assigning a weight to the open field ranging from 65% to 80%.



**Figure 12.** Per cent volume covered by at least 95% of the prescribed dose for plans having different weights of the open field and different patient motion amplitudes.

#### 4. Conclusions

Direct aperture optimization is a useful inverse planning technique for breast IMRT using tangential fields. With this approach, the benefits of an open flash segment are maintained while a uniform breast dose is achieved using IMRT. Typically, less than eight apertures per field are sufficient to generate a quality plan meaning that the plans can be delivered efficiently. In addition, our study on the impact of breathing motion on plan quality has demonstrated that when the weight of the open field exceeds 80%, the coverage is not sufficient for the plans to be acceptable even without considering the patient motion under the optimization constraints set so as to make sure that the hotspots for all plans are acceptable. All weights below 85% generate a high-quality plan when the patient motion is not taken into account. When the weight decreases below 65%, a 1 cm breast motion can cause excessive underdosage leading to an unacceptable plan. The optimum weight of the open field was found to be in the range of 65% to 80%.

#### Acknowledgments

The authors would like to thank Prowess, Inc. for its support and technical assistance.

#### References

- Buchholz T A, Gurgoze E, Bice W S and Prestidge B R 1997 Dosimetric analysis of intact breast irradiation in off-axis planes *Int. J. Radiat. Oncol. Biol. Phys.* **39** 261–7
- Cheng C W, Das I J and Baldassarre S 1994 The effect of the number of computed tomographic slices on dose distributions and evaluation of treatment planning systems for radiation therapy of intact breast *Int. J. Radiat. Oncol. Biol. Phys.* **30** 183–95
- Earl M A, Shepard D M, Naqvi S, Li X A and Yu C X 2003 Inverse planning for intensity-modulated arc therapy using direct aperture optimization *Phys. Med. Biol.* **48** 1075–89

- Frazier R C, Vicini F A, Sharpe M B, Remouchamps V M, Yan M, Fayad J, Baglan K L, Kestin L L, Martinez A A and Wong J W 2004 The impact of respiration on whole breast radiotherapy: a dosimetric analysis using active breathing control *Int. J. Radiat. Oncol. Biol. Phys.* **58** 1041–7
- George R, Keall P J, Kini V R, Vedam S S, Siebers J V, Wu Q, Lauterbach M H, Arthur D W and Mohan R 2003 Quantifying the effect of intrafraction motion during breast IMRT planning and dose delivery *Med. Phys.* **30** 552–62
- Keall P J, Kini V R, Vedam S S and Mohan R 2001 Motion adaptive x-ray therapy: a feasibility study *Phys. Med. Biol.* **46** 1–10
- Kestin L L, Sharpe M B, Franzier R C, Vicini F A, Yan D, Matter R C, Martinez A A and Wong J W 2000 Intensity modulation to improve dose uniformity with tangential breast radiotherapy: initial clinical experience *Int. J. Radiat. Oncol. Biol. Phys.* **48** 1559–68
- Kubo H D and Hill B C 1996 Respiration gated radiotherapy treatment: a technical study *Phys. Med. Biol.* **41** 83–91
- Langen K M and Jones D T L 2001 Organ motion and its management *Int. J. Radiat. Oncol. Biol. Phys.* **50** 265–78
- Li J S, Freedman G M, Price R, Wang L, Anderson P, Chen L, Xiong W, Yang J, Pollack A and Ma C-M 2004 Clinical implementation of intensity-modulated tangential beam irradiation for breast cancer *Med. Phys.* **31** 1023–31
- Lujan A E, Larsen E W, Balter J M and Kaken R K T 1999 A method for incorporating organ motion due to breathing into 3D dose calculation *Med. Phys.* **26** 715–20
- Mayo C S, Urie M M and Fitzgerald T J 2005 Hybrid IMRT plans—concurrently treating conventional and IMRT beams for improved breast irradiation and reduced planning time *Int. J. Radiat. Oncol. Biol. Phys.* **61** 922–32
- Naqvi S A, Earl M A and Shepard D M 2003 Convolution/superposition using the Monte Carlo method *Phys. Med. Biol.* **48** 2101–21
- Naqvi S A and D'Souza W D 2005 A stochastic convolution/superposition method with isocenter sampling to evaluate intrafraction motion effects in IMRT *Med. Phys.* **32** 1156–63
- Ozhasoglu C and Murphy M J 2002 Issues in respiratory motion compensation during external-beam radiotherapy *Int. J. Radiat. Oncol. Biol. Phys.* **52** 1389–99
- Remouchamps V M, Vicini F A, Martinez A A, Sharpe M B, Yan D, Kestin L L and Wong J W 2003a Significant reductions in heart and lung doses using deep inspiration breath hold with active breathing control and intensity-modulated radiation therapy for patients treated with locoregional breast irradiation *Int. J. Radiat. Oncol. Biol. Phys.* **55** 392–406
- Remouchamps V M, Letts N, Vicini F A, Sharpe M B, Kestin L L, Chen P Y, Martinez A A and Wong J W 2003b Initial clinical experience with moderate deep inspiration breath hold using an active breathing control device in the treatment of patients with left-sided breast cancer using external beam radiation therapy *Int. J. Radiat. Oncol. Biol. Phys.* **56** 704–15
- Remouchamps V M, Letts N, Vicini F A, Zielinski J A, Liang J, Kestin L L, Martinez A A and Wong J W 2003c Three dimensional evaluation of intra- and inter-fraction reproducibility of lung immobilization using active breathing control *Int. J. Radiat. Oncol. Biol. Phys.* **57** 968–78
- Shepard D M, Earl M A, Li X A, Naqvi S A and Yu C X 2002 Direct aperture optimization: a turnkey solution for step-and-shoot IMRT *Med. Phys.* **29** 1007–18
- Vicini F A, Sharpe M, Kestin L L, Wong J W, Remouchamps V M and Martinez A A 2004 The use of intensity modulated radiation therapy in the treatment of breast cancer: evolving definition, misdirected criticism, and untoward effects *Int. J. Radiat. Oncol. Biol. Phys.* **58** 1642–4
- Wilson E M, Williams F J, Lyn B E, Wong J W and Aird E G A 2003 Validation of active breathing control in patients with non-small-cell lung cancer to be treated with CHARTWEL *Int. J. Radiat. Oncol. Biol. Phys.* **57** 864–74
- Wong J W, Sharpe M B, Jaffray D V, Kini V R, Robertson J M, Stromberg J S and Martinez A A 1999 The use of active breathing control (ABC) to reduce margin for breathing motion *Int. J. Radiat. Oncol. Biol. Phys.* **44** 911–9
- Xing L, Crooks S, Li J G, Ozhasoglu C, Chen Y, Metha V, Goffinet D, Beavis A and Boyer A 2000 Incorporating respiratory motion into the design of intensity maps in IMRT treatment of breast cancer (abstract) *Int. J. Radiat. Oncol. Biol. Phys.* **48** 199
- Yu C Y, Jaffray D A and Wong J W 1998 The effects of intra-fraction organ motion on the delivery of dynamic intensity modulation *Phys. Med. Biol.* **43** 91–104